ResearchGate

See discussions, stats, and author profiles for this publication at: https://www.researchgate.net/publication/11925060

Model-Free Approach to the Dynamic Interpretation of Residual Dipolar Couplings in Globular Proteins

ARTICLE *in* JOURNAL OF THE AMERICAN CHEMICAL SOCIETY · JULY 2001

Impact Factor: 12.11 · DOI: 10.1021/ja010002z · Source: PubMed

CITATIONS
231

READS
17

5 AUTHORS, INCLUDING:

Jens Meiler
Vanderbilt University
235 PUBLICATIONS **5,854** CITATIONS
SEE PROFILE

Jeanine J Prompers
Technische Universiteit Eindhoven
74 PUBLICATIONS **1,523** CITATIONS
SEE PROFILE

Available from: Jeanine J Prompers
Retrieved on: 16 January 2016

Model-Free Approach to the Dynamic Interpretation of Residual Dipolar Couplings in Globular Proteins

Jens Meiler,[†] Jeanine J. Prompers,[‡] Wolfgang Peti,[†] Christian Griesinger,*[,†,§] and Rafael Brüschweiler*[,‡]

Contribution from the Institut für Organische Chemie, Universität Frankfurt, Marie-Curie-Strasse 11, D-60439 Frankfurt am Main, Germany, Gustaf H. Carlson School of Chemistry and Biochemistry, Clark University, 950 Main Street, Worcester, Massachusetts 01610-1477, and Max-Planck Institute for Biophysical Chemistry, Am Fassberg 11, D-37077 Göttingen, Germany

Received January 2, 2001. Revised Manuscript Received March 28, 2001

Abstract: The effects of internal motions on residual dipolar NMR couplings of proteins partially aligned in a liquid-crystalline environment are analyzed using a 10 ns molecular dynamics (MD) computer simulation of ubiquitin. For a set of alignment tensors with different orientations and rhombicities, MD-averaged dipolar couplings are determined and subsequently interpreted for different scenarios in terms of effective alignment tensors, average orientations of dipolar vectors, and intramolecular reorientational vector distributions. Analytical relationships are derived that reflect similarities and differences between motional scaling of dipolar couplings and scaling of dipolar relaxation data (NMR order parameters). Application of the self-consistent procedure presented here to dipolar coupling measurements of biomolecules aligned in different liquid-crystalline media should allow one to extract in a "model-free" way average orientations of dipolar vectors and specific aspects of their motions.

1. Introduction

Since the first measurements of nuclear dipolar spin−spin couplings in proteins caused by the partial alignment of the proteins with respect to the external magnetic field,[1−5] these parameters have become widely used for the determination and refinement of structures of biomolecules in solution.[6−11] While in most applications residual dipolar couplings (rdc) are interpreted in the context of a static structure, it has been suggested from early on that these couplings also probe protein dynamics.[12] In multimodular systems, such as multidomain proteins and complex sugars, differences in alignment tensors determined for individual domains were attributed to differential motions between the domains.[13−17]

In the context of biomolecular structure determination, dipolar couplings are used to refine structures by optimizing agreement between experimental couplings, D_j^{exp}, and dipolar couplings predicted from the structural model, D_j^{calc}. A commonly used measure for the agreement is the Q value, defined by[18]

$$Q = \frac{\sum_j (D_j^{\mathrm{exp}} - D_j^{\mathrm{calc}})^2}{\sum_j (D_j^{\mathrm{exp}})^2} \qquad (1)$$

The smaller Q, the better is the agreement between the structural model and the experimental data. In case of perfect agreement ($Q = 0$), $D_j^{\mathrm{exp}} = D_j^{\mathrm{calc}}$ for all j (values of Q larger than 1 are of little interest, since $Q = 1$ can always be achieved by setting $D_j^{\mathrm{calc}} = 0$). In our experience, Q values for dipolar couplings determined directly from X-ray structures and NMR structures determined without the use of dipolar couplings typically lie between 0.2 and 0.5.[18,19] Possible reasons for Q values deviating from zero are experimental uncertainties, dynamic and exchange

* To whom correspondence should be addressed. C.G.: phone +49 69 7982-9130, fax +49 69 7982 9128, E-mail cigr@mpibpc.mpg.de. R.B.: phone (508) 793-7220, fax (508) 793-8861, E-mail bruschweiler@nmr.clarku.edu.

[†] Universität Frankfurt.

[‡] Clark University.

[§] Max-Planck Institute for Biophysical Chemistry.

(1) Tolman, J. R.; Flanagan, J. M.; Kennedy, M. A.; Prestegard, J. H. *Proc. Natl. Acad. Sci. U.S.A.* **1995**, *92*, 9279−9283.

(2) Kung, H. C.; Wang, K. Y.; Goljer, I.; Bolton, P. H. *J. Magn. Reson. B* **1995**, *109*, 323−325.

(3) Tjandra, N.; Grzesiek, S.; Bax, A. *J. Am. Chem. Soc.* **1996**, *118*, 6264−6272.

(4) Tjandra, N.; Bax, A. *Science* **1997**, *278*, 1111−1114.

(5) Bax, A.; Tjandra, N. *J. Biomol. NMR* **1997**, *10*, 289−292.

(6) Bewley, C. A.; Gustafson, K. R.; Boyd, M. R.; Covell, D. G.; Bax, A.; Clore, G. M.; Gronenborn, A. M. *Nat. Struct. Biol.* **1998**, *5*, 571−578.

(7) Cai, M.; Huang, Y.; Zheng, R.; Wei, S.-Q.; Ghirlando, R.; Lee, M. S.; Craigie, R.; Gronenborn, A. M.; Clore, G. M. *Nat. Struct. Biol.* **1998**, *5*, 903−909.

(8) Clore, G. M.; Starich, M. R.; Bewley, C. A.; Cai, M.; Kuszewski, J. *J. Am. Chem. Soc.* **1999**, *121*, 6513−6514.

(9) Drohat, A. C.; Tjandra, N.; Baldisseri, D. M.; Weber, D. J. *Protein Sci.* **1999**, *8*, 800−809.

(10) Mollova, E. T.; Hansen, M. R.; Pardi, A. *J. Am. Chem. Soc.* **2000**, *122*, 11561−11562.

(11) Hus, J. C.; Marion, D.; Blackledge, M. *J. Am. Chem. Soc.* **2001**, *123*, 1541−1542.

(12) Tolman, J. R.; Flanagan, J. M.; Kennedy, M. A.; Prestegard, J. H. *Nat. Struct. Biol.* **1997**, *4*, 292−297.

(13) Weaver, J. L.; Prestegard, J. H. *Biochemistry* **1998**, *37*, 116−128.

(14) Fischer, M. W. F.; Losconczi, J. A.; Weaver, J. L.; Prestegard, J. H. *Biochemistry* **1999**, *38*, 9013−9022.

(15) Skrynnikov, N.; Goto, N. K.; Yang, D.; Choy, W.-Y.; Tolman, J. R.; Mueller, G. A.; Kay, L. E. *J. Mol. Biol.* **2000**, *295*, 1265−1273.

(16) Neubauer, H.; Meiler, J.; Peti, W.; Griesinger, C. *Helv. Chim. Acta* **2001**, *84*, 243−258.

(17) Tian, F.; Al-Hashimi, H. M.; Craighead, J. L.; Prestegard, J. H. *J. Am. Chem. Soc.* **2001**, *123*, 485−492.

(18) Cornilescu, G.; Marquardt, J. L.; Ottiger, M.; Bax, A. *J. Am. Chem. Soc.* **1998**, *120*, 6836−6837.

(19) Meiler, J.; Peti, W.; Griesinger, C. *J. Biomol. NMR* **2000**, *17*, 283−294.

10.1021/ja010002z CCC: $20.00 © 2001 American Chemical Society
Published on Web 05/26/2001

effects, and errors in the 3D structures, for example due to crystal packing in X-ray structures. NMR structures that are refined using dipolar couplings typically exhibit Q values between 0.05 and 0.3, depending also on the quality of the experimental data.[19,20]

In this work we investigate the effects of motions on Q values of backbone dipolar couplings using a 10 ns molecular dynamics (MD) simulation of ubiquitin and discuss several different scenarios for the structural and dynamic interpretation of dipolar couplings that explicitly take dynamics contributions into account. A practical procedure for including certain aspects of dynamics is the division of each dipolar coupling value by the corresponding Lipari−Szabo order parameter, S_{LS}, obtained from NMR relaxation experiments.[21] This procedure is valid only to a first-order approximation.[22] The quality of this approximation is quantitatively assessed here using the MD simulation as a reference from which averaged dipolar couplings as well as S_{LS} order parameters are computed and compared with each other. The inverse problem is then addressed to directly extract information on biomolecular structure and motions from dipolar couplings measured in multiple liquid-crystalline environments that give rise to different alignments. The proposed treatment is based on the assumptions that the structure and intramolecular motion are not significantly altered by the liquid-crystalline environment and that the alignment process is not affected by intramolecular motions. The treatment allows the determination of residual dipolar coupling order parameters, S_{rdc}, that probe motion up to the millisecond range and thus are complementary to the relaxation-derived Lipari−Szabo order parameters S_{LS}. We do not discuss here larger scale dynamics of (partially) unfolded proteins or interdomain dynamics of multidomain proteins. In the following section, the theoretical background of motional averaging effects on dipolar couplings is developed. In subsequent sections the theory is applied to the MD trajectory.

2. Motional Averaging of Dipolar Couplings

The residual dipolar couplings, which give rise to resonance splittings, result from the secular part of the magnetic dipole−dipole interactions between nuclear spins of molecules that are partially aligned in an anisotropic liquid. The dipolar splitting $\langle D\rangle$ (in units of hertz) between directly bonded heteronuclei X and H can be expressed in the laboratory frame as

$$\langle D\rangle = -\frac{\mu_0}{4\pi^2}\gamma_X\gamma_H\frac{h}{2\pi}(4\pi/5)^{1/2}\langle r_{XH}{}^{-3}\rangle\,\langle P_2(\cos\chi)\rangle \qquad (2)$$

where $P_2(\cos\chi) = (3\cos^2\chi - 1)/2$, χ is the angle of the internuclear vector to the external B_0 field, $\mu_0/4\pi = 10^{-7}$ V·s/A·m, γ_X, γ_H are the gyromagnetic ratios, and r_{XH} is the distance between the two spins. The angular brackets denote an ensemble average over orientations χ and distances r_{XH} or, assuming that the system is ergodic, a time average over a single molecule. In eq 2, it is assumed that radial and angular averaging are statistically separable, as is the case for directly bonded N−H and C−H atom pairs. Furthermore, the radial part $\langle r_{XH}{}^{-3}\rangle$ can often be considered to be identical for nuclear X−H pairs of the same kind.

For an internally static molecule, the dipolar couplings can alternatively be expressed in a molecular fixed frame in terms of a traceless reduced alignment tensor **D** (in units of hertz), with eigenvalues D_{xx}, D_{yy}, and D_{zz}, where $|D_{zz}| \geq |D_{yy}| \geq |D_{xx}|$.[22] In the eigenframe of this tensor, the dipolar coupling between two nuclei connected by an internuclear vector with orientation $\Omega = (\theta,\varphi)$, where θ,φ denote the polar angles in the eigenframe of **D**, is given by D_{stat}:[22]

$$D_{stat} = D_a\left\{3\cos^2\theta - 1 + \frac{3}{2}R\sin^2\theta\cos 2\varphi\right\} \qquad (3)$$

where $D_a = D_{zz}/2$ is the axial component and $R = {}^2/_3(D_{xx} - D_{yy})/D_{zz}$ is the rhombicity of **D** with $0 \leq R \leq {}^2/_3$. If **D** is symmetric, D_{zz} corresponds to the principal axis value along the symmetry axis of **D**. For a given alignment tensor **D**, D_{zz} is the largest coupling possible for the considered type of X−H spin pairs.

In the presence of intramolecular molecular dynamics, the experimental dipolar coupling corresponds to a conformational average, denoted by angular brackets, relative to the alignment tensor frame:

$$\langle D\rangle = D_a\left\{\langle 3\cos^2\theta - 1\rangle + \frac{3}{2}R\langle\sin^2\theta\cos 2\varphi\rangle\right\} \qquad (4)$$

Equation 4 assumes that intramolecular motion does not interfere with the alignment process, i.e., that the alignment process is not significantly affected by internal motions. In the case of an alignment process due to steric effects,[23] this condition is fulfilled for motions that do not much alter the shape of the molecule. For small-amplitude, short-range motions, which can have a local or a concerted character,[24] eq 4 is expected to be more accurate than for larger amplitude motions of loops and termini, for example.

It is useful to express eq 4 in terms of normalized second-order spherical harmonic functions $Y_{2M}(\theta,\varphi)$:[15]

$$\frac{\langle D\rangle}{D_{zz}} = \sqrt{\frac{4\pi}{5}}\left(\langle Y_{20}(\theta,\varphi)\rangle + \sqrt{\frac{3}{8}}R(\langle Y_{22}(\theta,\varphi)\rangle + \langle Y^*_{22}(\theta,\varphi)\rangle)\right) \qquad (5)$$

where $Y_{20}(\theta,\varphi) = \sqrt{5/(16\pi)}(3\cos^2\theta - 1)$, $Y_{2\pm2}(\theta,\varphi) = \sqrt{15/(32\pi)}\,e^{\pm2i\varphi}\sin^2\theta$.[25] In what follows, $Y_{2\pm1}(\theta,\varphi) = \mp\sqrt{15/(8\pi)}\,e^{\pm i\varphi}\cos\theta\sin\theta$ will also be used.

In analogy to eq 3, D_{stat} can be defined for reference purposes as the dipolar coupling expected from a static internuclear vector pointing along the average orientation $(\theta_{av},\varphi_{av}) = (\langle\theta\rangle,\langle\varphi\rangle)$:

$$\frac{D_{stat}}{D_{zz}} = \sqrt{\frac{4\pi}{5}}\left(Y_{20}(\theta_{av},\varphi_{av}) + \sqrt{\frac{3}{8}}R(Y_{22}(\theta_{av},\varphi_{av}) + Y^*_{22}(\theta_{av},\varphi_{av}))\right) \qquad (6)$$

The effect of intramolecular reorientational motion on the dipolar coupling can be expressed by the *dipolar scaling factor*, λ_{rdc}:

$$\lambda_{rdc} = \langle D\rangle/D_{stat} \qquad (7)$$

In the absence of motion, $\lambda_{rdc} = 1$, and in the presence of motion, $-\infty < \lambda_{rdc} < \infty$.

(20) Ottiger, M.; Bax, A. *J. Am. Chem. Soc.* **1998**, *120*, 12334−12341.
(21) Lipari, G.; Szabo, A. *J. Am. Chem. Soc.* **1982**, *104*, 4546−4559.
(22) Clore, G. M.; Gronenborn, A. M.; Bax, A. *J. Magn. Reson.* **1998**, *133*, 216−221.
(23) Zweckstetter, M.; Bax, A. *J. Am. Chem. Soc.* **2000**, *122*, 3791−3792.
(24) Brüschweiler, R. *J. Chem. Phys.* **1995**, *102*, 3396−3403.
(25) Zare, R. N. *Angular Momentum*; John-Wiley & Sons: New York, 1988.

A benefit of eq 5 is that it can be easily transformed into a new reference frame related to the old reference frame by a three-dimensional rotation $\mathbf{R}(\alpha,\beta,\gamma)$ using the well-known transformation properties of the spherical harmonics $Y_{2M}(\theta,\varphi)$ under a three-dimensional rotation specified by the Euler angles α, β, and γ:[25]

$$\mathbf{R}(\alpha,\beta,\gamma)Y_{2M}(\theta,\varphi) = \sum_{M'=-2}^{2} e^{-i\alpha M'} d^{(2)}_{M'M}(\beta)\, e^{-i\gamma M}\, Y_{2M'}(\theta,\varphi) \tag{8}$$

Provided that the average protein structure and the dynamics do not vary with different alignment media, it follows that the dipolar coupling $\langle D\rangle$ measured in a new alignment frame i with axial component $D_{zz}^{(i)}$ and rhombicity $R^{(i)}$ that is related to the old frame by the rotation $\mathbf{R}(\alpha^{(i)},\beta^{(i)},\gamma^{(i)})$ can be expressed as

$$\frac{\langle D^{(i)}\rangle}{D_{zz}^{(i)}} = \sqrt{\frac{4\pi}{5}}\left(\sum_{M'=-2}^{2} e^{-iM'\alpha^{(i)}}\, d^{(2)}_{M'0}(\beta^{(i)})\langle Y_{2M'}\rangle\right) + \sqrt{\frac{4\pi}{5}}\sqrt{\frac{3}{8}}R\left(\sum_{M'=-2}^{2} e^{-iM'\alpha^{(i)}}\, d^{(2)}_{M'2}(\beta^{(i)})\, e^{-2i\gamma^{(i)}}\langle Y_{2M'}\rangle + e^{-iM'\alpha^{(i)}}\, d^{(2)}_{M'-2}(\beta^{(i)})\, e^{2i\gamma^{(i)}}\langle Y_{2M'}\rangle\right) \tag{9}$$

Note that eq 9 is linear in the five motionally averaged spherical harmonics $\langle Y_{2M'}(\theta,\varphi)\rangle$. If the couplings $\langle D^{(i)}\rangle$ belonging to a certain dipolar interaction are measured for five (or more) known alignments tensors $\{D_{zz}^{(i)}, R^{(i)}, \alpha^{(i)}, \beta^{(i)}, \gamma^{(i)}\}$, the five quantities $\langle Y_{2M'}\rangle$, $M' = -2, -1, 0, 1, 2$ belonging to this dipolar interaction can be determined by solving the linear system of equations of eq 9 using, for example, singular-value decomposition or Moore−Penrose inversion.[26] The average vector orientation $(\theta_{av},\varphi_{av})$ can be approximated by the effective orientation $(\theta_{eff},\varphi_{eff})$ that is found by minimizing the sum

$$\sum_{M=-2}^{2}\left(\langle Y_{2M}(\theta,\varphi)\rangle - Y_{2M}(\theta_{eff},\varphi_{eff})\right)^2 \tag{10}$$

To discuss the effects of symmetry in the motional distributions of an internuclear vector, it is useful to describe the distribution in a frame with the z axis pointing along the average orientation of the vector. In this new frame the instantaneous orientation of a vector is denoted by (θ',φ'). If $\langle e^{\pm i\varphi'}\rangle = \langle e^{\pm 2i\varphi'}\rangle = 0$, as is the case for axially symmetric reorientational motion, it follows $\langle Y_{2M'}\rangle = 0$ except for $\langle Y_{20}\rangle$. To calculate the dipolar coupling, a coordinate transformation into the alignment frame is necessary, which is achieved by the rotation $\mathbf{R}'(\alpha' = 0, \beta' = -\theta_{av}, \gamma' = -\varphi_{av})$.

The extent of *nonaxial symmetry* of the motion can be quantified by the *motional asymmetry parameter* η fulfilling $0 \le \eta \le 1$:

$$\eta = \left(\frac{\sum_{M=\pm1,\pm2}\langle Y_{2M}(\theta',\varphi')\rangle\langle Y^*_{2M}(\theta',\varphi')\rangle}{\sum_{M=0,\pm1,\pm2}\langle Y_{2M}(\theta',\varphi')\rangle\langle Y^*_{2M}(\theta',\varphi')\rangle}\right)^{1/2}$$

$$= \frac{(S^2 - \langle P_2(\cos\theta')\rangle^2)^{1/2}}{S} \tag{11}$$

where the generalized S^2 order parameter has been introduced, which plays a key role in the "model-free" interpretation of heteronuclear NMR spin relaxation data by Lipari and Szabo,[21]

$$S^2 = \frac{4\pi}{5}\sum_{M=-2}^{2}\langle Y_{2M}(\theta,\varphi)\rangle\langle Y^*_{2M}(\theta,\varphi)\rangle \tag{12}$$

The S^2 order parameter extracted from spin relaxation data is sensitive to motions faster than the overall tumbling correlation time and is denoted here as S^2_{LS}. In contrast, an S^2 order parameter can be determined from residual dipolar couplings using eqs 9 and 12, which probes the much wider submillisecond time scale range and which is denoted as S^2_{rdc}. Therefore, S^2_{LS} is an upper limit for S^2_{rdc}, $S^2_{rdc} \le S^2_{LS}$. Note that when using the 10 ns MD trajectory for calculating S^2_{LS} and S^2_{rdc}, the two parameters probe the same time scales and are therefore identical.

For *axially symmetric motion* with respect to the average orientation $(\theta_{av},\varphi_{av})$, for which $\langle e^{\pm i\varphi'}\rangle$ and $\langle e^{\pm 2i\varphi'}\rangle$ vanish, the average dipolar coupling $\langle D\rangle$ can be expressed in a more compact way. Using eq 9 with $\langle Y_{2M'}(\theta',\varphi')\rangle = 0$ for $M' = \pm1, \pm2$ it follows

$$\frac{\langle D\rangle_{sym}}{D_{zz}} = \sqrt{\frac{4\pi}{5}}\langle Y_{20}(\theta',\varphi')\rangle\left(d^{(2)}_{00}(\beta') + \sqrt{\frac{3}{8}}R(d^{(2)}_{02}(\beta')\, e^{-2i\gamma'} + d^{(2)}_{0-2}(\beta')\, e^{2i\gamma'})\right)$$

$$= \left\langle\frac{1}{2}(3\cos^2\theta' - 1)\right\rangle\left(\frac{1}{2}(3\cos^2\beta' - 1) + \frac{3}{4}R\sin^2\beta'\cos 2\gamma'\right) \tag{13}$$

where $\beta' = -\theta_{av}$, $\gamma' = -\varphi_{av}$. Consequently, the dipolar coupling of an internuclear vector is scaled under axially symmetric motion as compared to a static vector pointing along the average direction by

$$\lambda_{rdc,sym} = \frac{\langle D\rangle_{sym}}{D_{stat}} = \langle P_2(\cos\theta')\rangle \tag{14}$$

where θ' is the angle between an instantaneous internuclear vector and the average vector orientation $(\theta_{av},\varphi_{av})$. Note that $\lambda_{rdc,sym}$ does not depend on the relative orientation $(\theta_{av},\varphi_{av})$ with respect to the alignment frame. In the case of axially symmetric motion, S^2_{rdc} simplifies to $S^2_{rdc,sym} = (4\pi/5)\langle Y_{20}(\theta',\varphi')\rangle^2 = \langle P_2(\cos\theta')\rangle^2$ and thus

$$\lambda_{rdc,sym} = S_{rdc,sym} \tag{15}$$

From eq 14 follows that $-0.5 \le \lambda_{rdc,sym}, S_{rdc,sym} \le 1$.

Knowledge of λ_{rdc} is useful for the determination of an average 3D protein structure using residual dipolar couplings. D_{stat} values, which are directly related to $(\theta_{av},\varphi_{av})$ by eq 6, could then be obtained by dividing experimental couplings $\langle D\rangle$ by λ_{rdc} according to eq 7. Since in practice λ_{rdc} values are not readily available, they sometimes are approximated by their respective S_{LS} values extracted from spin relaxation experiments.[18] $\lambda_{rdc} = S_{LS}$ holds if (i) internal reorientational motion is axially symmetric and (ii) all relevant motions take place on nanosecond and subnanosecond time scales. Condition (i) can be tested by

(26) Press, W. H.; Flannery, B. P.; Teukolsky, S. A.; Vetterling, W. T. *Numerical Recipes in C*; Cambridge University Press: Cambridge, 1988.

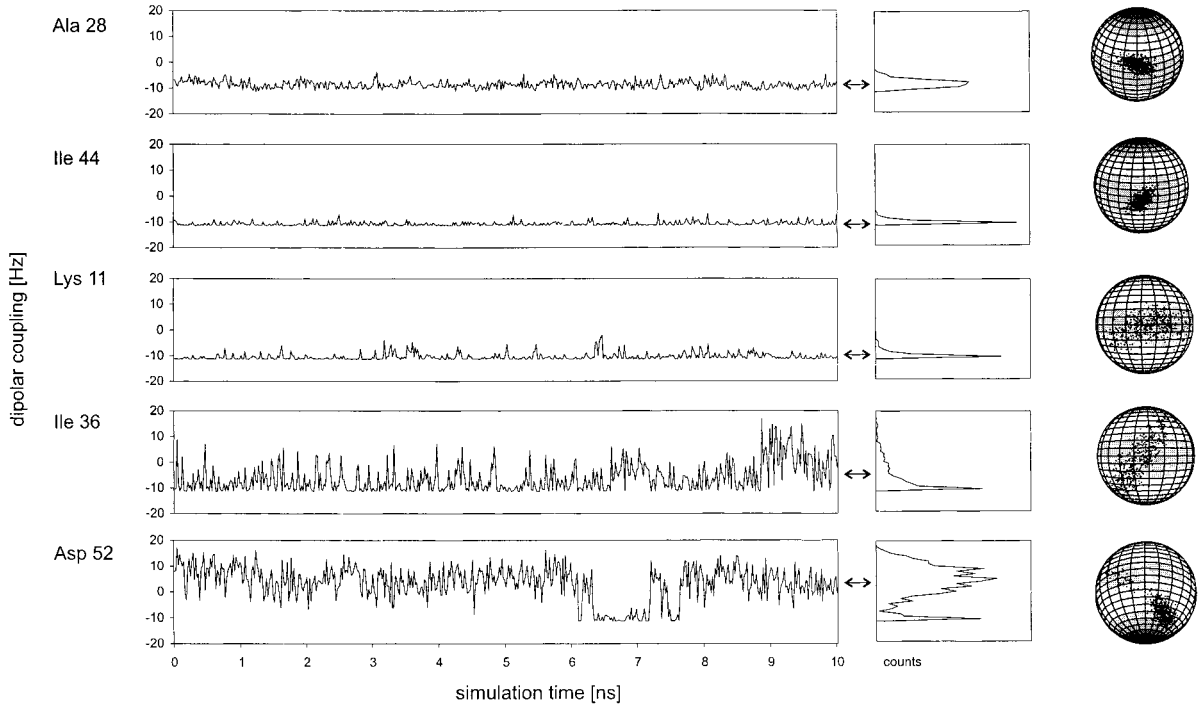

Figure 1. Time dependence of $^{15}N-^{1}H^{N}$ residual dipolar coupling values for selected amino acids of ubiquitin extracted from a 10 ns molecular dynamics (MD) simulation. Ala 28 belongs to the α helix, Ile 44 to a β strand, and Lys 11, Ile 36, Asp 52 to loop regions. In the middle, the distributions of the couplings are plotted vertically, with the horizontal arrows indicating average dipolar coupling values that would be observed experimentally. The dots plotted on the surface of the spheres (right) correspond to the $N-H^{N}$ orientations sampled during the MD trajectory (500 snapshots).

using a molecular dynamics (MD) simulation, which is done in the following section. Presently, condition (ii) can be assessed only by comparison with experimental data. If condition (i) is fulfilled but (ii) is not fulfilled, $S_{LS,sym}$ represents an upper limit, $\lambda_{rdc,sym} = S_{rdc,sym} \leq S_{LS,sym}$.

In addition, it was assumed here that the alignment tensor **D** is a priori known. In practice, however, **D** is iteratively adjusted during structure refinement based on residual dipolar couplings. Thus, the best fitting alignment tensor **D** implicitly includes certain motional contributions. In the following, a 10 ns MD simulation of ubiquitin is used to elucidate the influence of molecular motion on the interpretation of residual dipolar couplings.

3. Dipolar Couplings Calculated from MD Trajectory

A MD simulation of native ubiquitin was carried out under periodic boundary conditions using the program CHARMM 24.[27,28] An energy-minimized all-atom representation of the X-ray structure of ubiquitin[29] was embedded in a cubic box with a side length of 46.65 Å, containing a total of 2909 explicit water molecules. The simulation was performed at a temperature of 300 K with an integration time step of 1 fs. Details of this simulation have been reported elsewhere.[30] During a simulation time of 11 ns, snapshots were stored every 500 fs. From a 10 ns section of the trajectory, covering the range between 1 and 11 ns, 500 snapshots were selected with an increment of 20 ps for calculating dipolar couplings.

The 500 snapshots were reoriented and translated with respect to the snapshot at 6 ns by a least-squares superposition of their backbone atoms belonging to regular secondary structures. An average structure was constructed from the 500 reoriented snapshots by averaging over the Cartesian coordinates of all heavy atoms. The average positions of hydrogen atoms were determined by adding averaged X−H vectors (X = N or C atoms), which were rescaled to their standard lengths (1.02 Å for N−H and 1.09 Å for C−H), to the position of the corresponding X atom.

The shape of ubiquitin undergoes only small changes during the trajectory, as was assessed by computing inertia tensors for the 500 snapshots. The standard deviations of the moments of inertia tensor lie between 1% and 2%, which supports the validity of the assumptions underlying eq 4. It is assumed in the following that the MD trajectory represents a realistic description of the internal dynamics of ubiquitin, and thus slower time scale motions, which are not represented by the 10 ns simulation, are ignored.

To characterize the effect of dynamics, dipolar couplings were calculated from the 500 snapshots for a fixed alignment tensor **D** with $D_{zz} = 20$ Hz (with respect to $^{15}N-^{1}H^{N}$ couplings), $R = 0$, $\alpha = \beta = \gamma = 0$. The time dependence of backbone $^{15}N-^{1}H^{N}$ couplings is depicted in Figure 1 for a selection of five amino acids that experience variable amounts of motion: Ala 28 (α helix), Ile 44 (β sheet), Lys 11 (loop), Ile 36 (loop), and Asp 52 (loop). Also given in Figure 1 are the distributions of the dipolar couplings over the trajectory. Most of the displayed distributions, which also depend on the size and orientation of the alignment tensor, show quasi-singularities and are unimodal

(27) Brooks, R. B.; Bruccoleri, R. E.; Olafson, B. D.; States, D. J.; Swaminathan, S.; Karplus, M. *J. Comput. Chem.* **1983**, *4*, 187−217.

(28) MacKerell, A. D., Jr.; Bashford, D.; Bellott, M.; Dunbrack, R. L., Jr.; Evanseck, J. D.; Field, M. J.; Fischer, S.; Gao, J.; Guo, H.; Ha, S.; Joseph-McCarthy, D.; Kuchnir, L.; Kuczera, K.; Lau, F. T. K.; Mattos, C.; Michnick, S.; Ngo, T.; Nguyen, D. T.; Prodhom, B.; Reiher, W. E., III; Roux, B.; Schlenkrich, M.; Smith, J. C.; Stote, R.; Straub, J.; Watanabe, M.; Wiórkiewicz-Kuczera, J.; Yin, D.; Karplus, M. *J. Phys. Chem. B* **1998**, *102*, 3586−3616.

(29) Vijay-Kumar, S.; Bugg, C. E.; Cook, W. J. *J. Mol. Biol.* **1987**, *194*, 531−544.

(30) Lienin, S. F.; Bremi, T.; Brutscher, B.; Brüschweiler, R.; Ernst, R. R. *J. Am. Chem. Soc.* **1998**, *120*, 9870−9879.

Table 1. Back-Calculated Alignment Tensors and *Q* Values for Ubiquitin According to Scenario I (No Scaling)

nuclei[a]		$(\tilde{D}_{zz}/D_{zz})$[b]	*R*[c]	α[d] (deg)	β[e] (deg)	γ[f] (deg)	Q_{all}[g]	Q_{sec}[h]	Q_{loop}[i]
true		1.00	0.00	0	0	0	0.00	0.00	0.00
N	H^N	1.00	0.00	0	0	0	0.15	0.08	0.24
C^α	H^α	1.00	0.00	0	0	0	0.10	0.08	0.12
H^N	H^α	1.00	0.00	0	0	0	0.07	0.04	0.09
true		1.00	0.33	0	0	0	0.00	0.00	0.00
N	H^N	1.00	0.33	0	0	0	0.16	0.08	0.22
C^α	H^α	1.00	0.33	0	0	0	0.09	0.07	0.11
H^N	H^α	1.00	0.33	0	0	0	0.07	0.04	0.09
true		1.00	0.67	0	0	0	0.00	0.00	0.00
N	H^N	1.00	0.67	0	0	0	0.16	0.09	0.23
C^α	H^α	1.00	0.67	0	0	0	0.10	0.08	0.11
H^N	H^α	1.00	0.67	0	0	0	0.07	0.04	0.09
N	H^N	1.00	0.00	0	0	0	0.15	0.08	0.24
		1.00	0.00	0	45	0	0.14	0.07	0.19
		1.00	0.00	0	45	90	0.12	0.09	0.15
		1.00	0.00	0	45	180	0.10	0.07	0.13
		1.00	0.00	0	45	270	0.14	0.08	0.18
		1.00	0.00	0	90	0	0.12	0.06	0.24
		1.00	0.00	0	90	45	0.09	0.07	0.14
		1.00	0.00	0	90	90	0.14	0.06	0.20
		1.00	0.00	0	90	135	0.16	0.08	0.26

[a] Pairs of nuclei for which dipolar couplings are computed. [b] Ratio of the best fitting and the predefined tensor size ($D_{zz} = 20$ Hz for $N-H^N$ couplings). [c] Rhombicities and [d,e,f] orientations of the predefined and back-calculated tensors. [g,h,i] Q_{all}, Q_{sec}, and Q_{loop} are the *Q* values (eq 1) for the whole protein, the secondary structural elements, and the loops, respectively.

except for Asp 52, where larger scale backbone modulations lead to a bimodal distribution.

4. Influence of Motion on *Q* Values

In practice, experimental dipolar couplings are commonly refined toward a single static structure. It is investigated here what level of agreement can be expected between experimental couplings and couplings calculated from the average structure in the presence of molecular motion occurring during the 10 ns MD trajectory of ubiquitin.

For the following analyses, sets of dipolar couplings belonging to 11 alignment tensors with different orientations and rhombicities were constructed from the 500 snapshots taken from the trajectory (see Table 1). Here and in the following, it is assumed that changes in the alignment tensor leave intramolecular motions unaffected. For three alignment tensors with $D_{zz} = 20$ Hz (for $N-H^N$ dipolar couplings) and *R* values set to 0, $^1/_3$, and $^2/_3$, respectively, dipolar couplings were computed for $N-H^N$, $C^\alpha-H^\alpha$, and H^N-H^α spin pairs. In addition, eight more alignment tensors with $R = 0$ and $D_{zz} = 20$ Hz were defined by reorienting the original tensor using rotation matrixes $\mathbf{R}(\alpha,\beta,\gamma)$ with the following Euler angles to sample a representative distribution of tensor orientations:

$$(\alpha,\beta,\gamma) = \{(0°,45°,0°), (0°,45°,90°), (0°,45°,180°), (0°,45°,270°), (0°,90°,0°), (0°,90°,45°), (0°,90°,90°), (0°,90°,135°)\}$$

For these eight alignment tensors, only $N-H^N$ couplings were computed.

On the basis of the MD simulation of ubiquitin, the effect of motion on *Q* was analyzed for three scenarios, I, II, and III, that involve different treatments of the data:

I. In this scenario, for a given alignment tensor, dipolar couplings were averaged over the 500 MD snapshots and compared with the dipolar couplings calculated from the average structure described in the previous section using the same alignment tensor.

II. In this scenario, for a given alignment tensor, dipolar couplings were averaged over the 500 MD snapshots and compared with the dipolar couplings calculated from the average structure using an optimized alignment tensor that was varied in size and orientation to minimize *Q*.

III. In this scenario, for a given alignment tensor, dipolar couplings were averaged over the 500 MD snapshots and subsequently divided by their respective S_{LS} order parameters calculated from the same snapshots. These rescaled dipolar couplings were then compared with the dipolar couplings calculated from the average structure using an optimized alignment tensor that was varied in size and orientation to minimize *Q*.

Scenario I corresponds to a situation where the "true" alignment tensor is known from external sources, for example theoretical calculations[23,31] or paramagnetic alignment. In this case, *Q* values become largest and motional effects are strongest, since they are not included in the form of a scaled alignment tensor. For scenario II, which is equivalent to overall scaling of all dipolar couplings combined with reorientation of the alignment tensor, readjustment of the alignment tensor can partially absorb internal motional effects. For example, if intramolecular motion reduces all dipolar couplings by 10% (compared to the couplings of the average structure), a new alignment tensor for the average structure that is 10% smaller would still yield $Q = 0$. This approach is equivalent to scaling of all couplings by a uniform λ_{rdc} value. Since the amplitudes of intramolecular motion generally vary between different protein sites, there will be no uniform scaling of dipolar couplings. Instead, individual motional scaling of dipolar couplings must be explicitly taken into account, which is the approach followed in scenario III. In the absence of any other information, a commonly used guess for the scaling factors are the S_{LS} order parameters of eq 12 obtained from spin relaxation measurements. As was shown in section 2 (eq 15), the scaling by S_{LS} values is adequate if all intramolecular motions are axially symmetric and take place on nanosecond and subnanosecond time scales that are accessed by spin relaxation experiments.

All three scenarios were analyzed for all 11 alignment tensors, and the results are compiled in Tables 1−3. For scenarios II and III, which involve fitting of the alignment tenors, the program DipoCoup[19] was used, performing a Moore−Penrose inversion, also known as singular-value decomposition,[26,32] previously used for the analysis of NMR relaxation data for anisotropic tumbling.[33] Since the results significantly differ between protein backbone parts with a well-defined secondary structure and loop regions, *Q* values were calculated for these different parts as well as for the whole protein backbone. Amino acids that belong to either a helix or a β sheet have residue numbers 2−7, 12−17, 23−34, 41−45, 49−50, and 65−72.

For scenario I, the *Q* values vary between 0.04 and 0.26 (see Table 1). They clearly depend on the type of vectors: $N-H^N$ vectors show *Q* values that are larger than those of $C^\alpha-H^\alpha$ vectors, which in turn have *Q* values that are larger than those of H^N-H^α vectors. This is not surprising since the H^N-H^α distances are longer than the one-bond distances, and thus a displacement of the H^N or H^α atom causes only a minor change

(31) Ferrarini, A.; Moro, G. J.; Nordio, P. L. *Mol. Phys.* **1992**, *77*, 1−15.
(32) Losonczi, J. A.; Andrec, M.; Fischer, M. W. F.; Prestegard, J. H. *J. Magn. Res.* **1999**, *138*, 334−342.
(33) Brüschweiler, R.; Liao, X.; Wright, P. E. *Science* **1995**, *268*, 886−889.

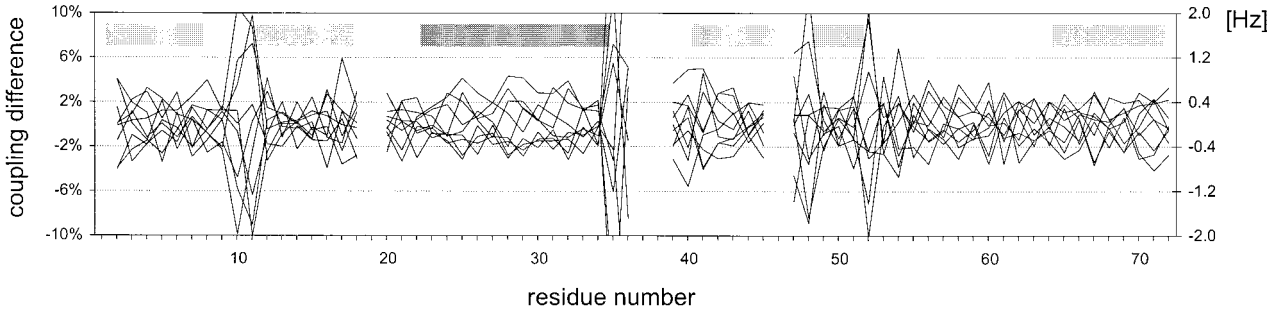

Figure 2. Differences between dipolar $N-H^N$ couplings averaged over the 500 MD snapshots of ubiquitin and the back-calculated couplings determined for the (static) $N-H^N$ vectors of the average structure as a function of residue number. The alignment tensor was optimized according to scenario II (see text). The calculation was done for each of the nine axially symmetric alignment tensors ($R = 0$) given in Table 2. The light gray bars on top of this figure (and also of Figures 3 and 6) indicates the β strands and the dark bar the α helix.

Table 2. Back-Calculated Alignment Tensors and Q Values for Ubiquitin According to Scenario II (Uniform Scaling)

nuclei[a]		$(\tilde{D}_{zz}/D_{zz})$[b]	R[c]	α[d] (deg)	β[e] (deg)	γ[f] (deg)	Q_{all}[g]	Q_{sec}[h]	Q_{loop}[i]	S_{LS}[j]
true		1.00	0.00	0	0	0	0.00	0.00	0.00	
N	H^N	0.90	0.04	0	0	0	0.10	0.05	0.17	0.91
C^α	H^α	0.92	0.01	0	1	0	0.06	0.04	0.07	0.94
H^N	H^α	0.95	0.01	0	−1	0	0.04	0.03	0.05	0.95
true		1.00	0.33	0	0	0	0.00	0.00	0.00	
N	H^N	0.89	0.33	0	0	−2	0.11	0.06	0.15	0.91
C^α	H^α	0.92	0.35	0	1	0	0.05	0.04	0.06	0.94
H^N	H^α	0.95	0.33	0	−1	0	0.04	0.03	0.05	0.95
true		1.00	0.67	0	0	0	0.00	0.00	0.00	
N	H^N	0.91	0.64	1	0	1	0.08	0.04	0.14	0.91
C^α	H^α	0.95	0.65	0	89	0	0.06	0.03	0.07	0.94
H^N	H^α	0.97	0.65	0	0	0	0.04	0.02	0.07	0.95
N	H^N	0.90	0.04	0	0	0	0.10	0.05	0.17	0.91
		0.91	0.03	0	45	0	0.09	0.05	0.13	0.91
		0.90	0.02	0	45	91	0.06	0.05	0.07	0.91
		0.92	0.01	0	45	180	0.06	0.03	0.08	0.91
		0.91	0.01	0	45	270	0.09	0.06	0.11	0.91
		0.91	0.02	0	90	1	0.08	0.04	0.16	0.91
		0.93	0.01	0	90	45	0.05	0.03	0.09	0.91
		0.90	0.02	0	90	90	0.10	0.06	0.13	0.91
		0.89	0.02	0	90	135	0.11	0.05	0.18	0.91

[a] Pairs of nuclei for which dipolar couplings are computed. [b] Ratio of the best fitting and the predefined tensor size ($D_{zz} = 20$ Hz for $N-H^N$ couplings). [c] Rhombicities and [d,e,f] orientations of the predefined and back-calculated tensors. [g,h,i] Q_{all}, Q_{sec}, and Q_{loop} are the Q values (eq 1) for the whole protein, the seconday structural elements, and the loops, respectively. [j] S_{LS} is the average order parameter for these vectors calculated from the MD trajectory according to eq 12.

in the vector orientation. The Q values depend on the orientation of the alignment tensor but they are nearly independent of R. Significant differences in Q are observed between regular secondary structures and loop regions.

The results of scenario II, which are summarized in Table 2, demonstrate the effect on Q values if the alignment tensor is allowed to vary. As compared to Table 1, the Q values drop by about 30%. The motional effects are contained in modified alignment tensors **D**. The directions of the principal axes change typically by less than 1°, and the rhombicity changes by 0.04 or less. The largest effects are seen in the new $\tilde{D}_{zz}$ values, which are scaled relative to the original D_{zz} values by factors between 0.89 and 0.95. Table 2 contains also average S_{LS} and S_{rdc} order parameters calculated from the 500 snapshots according to eq 12. The S_{LS} and S_{rdc} values vary between 0.91 and 0.95, which is comparable to the scaling factor variations $\tilde{D}_{zz}/D_{zz}$. The Q values depend on the details of the motional distributions and average orientations of the internuclear vectors relative to the alignment tensors. The Q values vary for the chosen alignment tensors by as much as a factor of 2. In Figure 2, the differences in back-calculated and "true" $N-H^N$ dipolar couplings are plotted as a function of the residue number for the nine alignment tensors with different orientations defined in the lower part of Table 2. For individual $N-H^N$ couplings, the motional influences characteristically depend on the directions sampled by the $N-H^N$ vector relative to the alignment tensor. In the absence of rhombicity, $R = 0$, motion has the strongest influence for the average directions $\theta_{av} = 0°, \pm 90°, 180°$, for which $P_2(\cos\theta)$ has maximal curvature. The differences between back-calculated and "true" couplings, which are distributed around zero, are largest for the loop regions that do not belong to regular secondary structure. $N-H^N$ vectors of these regions have calculated S^2 order parameters lower than 0.8 (see Supporting Information). For some but not all of these vectors, the orientational distributions have not converged during the 10 ns MD trajectory, which can also be seen for some of the examples shown in Figure 1. Figure 2 illustrates that the effect of dynamics on the observable dipolar coupling value depends on the orientation of the alignment tensor. The alignment tensor defines the projection along which motion is observable. The possibility to reconstruct characteristic motional features from dipolar couplings collected for different alignment tensors is discussed below.

For scenario III (Table 3), where the average dipolar couplings are individually divided by their S_{LS}, S_{rdc} values, the fitted alignment tensors almost identically reproduce the "true" alignment tensors with changes in R smaller than 0.03 and $\tilde{D}_{zz}$ values lying within 1% of D_{zz}. All Q values are further decreased as compared to the values in scenario II, with the largest reductions found for the mobile loop regions, where Q drops between 0.02 and 0.10. Figure 3 demonstrates the improved agreement for the individual $N-H^N$ pairs as compared to the case in Figure 2. However, the Q values can still significantly differ from zero (see Table 3): for $N-H^N$ dipolar couplings they vary between 0.04 and 0.07. This behavior is indicative of non-axially symmetric reorientational local motions of these internuclear vectors. Thus, the order parameter S_{LS}, S_{rdc} does not always accurately represent the motional scaling λ_{rdc} of dipolar couplings during the MD simulation. The residual discrepancies shown in Figure 3 are smallest for $N-H^N$ vectors belonging to regular secondary structures, where dynamics is smaller and more closely matches axial symmetry than in the loop regions, where more complicated motion occurs that is generally more asymmetric. Analogous analyses carried out for alignment tensors with increasing rhombicities R indicate that changes in R can also have non-negligible effects on dipolar couplings.

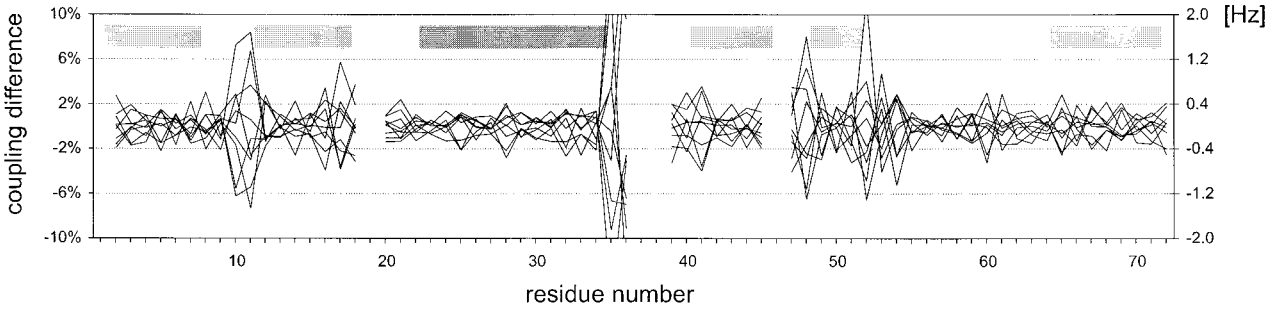

Figure 3. Differences between scaled dipolar $N-H^N$ couplings averaged over the 500 MD snapshots of ubiquitin and the back-calculated couplings determined for the (static) $N-H^N$ vectors of the average structure as a function of residue number. The dipolar couplings determined by averaging over the MD snapshots were scaled with their Lipari−Szabo order parameter S_{LS} according to scenario III. The calculation was done for each of the nine axially symmetric alignment tensors ($R = 0$) given in Table 3.

Table 3. Back-Calculated Alignment Tensors and Q Values for Ubiquitin According to Scenario III (Individual Scaling)

nuclei[a]		$(\tilde{D}_{zz}/D_{zz})$[b]	R[c]	α[d] (deg)	β[e] (deg)	γ[f] (deg)	Q_{all}[g]	Q_{sec}[h]	Q_{loop}[i]
true		1.00	0.00	0	0	0	0.00	0.00	0.00
N	H^N	0.99	0.03	0	0	0	0.07	0.04	0.11
C^α	H^α	1.00	0.00	0	0	0	0.02	0.02	0.02
H^N	H^α	1.00	0.01	0	−1	0	0.03	0.02	0.04
true		1.00	0.33	0	0	0	0.00	0.00	0.00
N	H^N	1.00	0.35	0	1	2	0.08	0.05	0.11
C^α	H^α	1.00	0.34	0	0	0	0.03	0.03	0.03
H^N	H^α	1.00	0.34	0	1	0	0.03	0.02	0.04
true		1.00	0.67	0	0	0	0.00	0.00	0.00
N	H^N	1.01	0.65	0	0	0	0.04	0.02	0.07
C^α	H^α	1.01	0.66	0	0	0	0.04	0.02	0.04
H^N	H^α	1.01	0.66	−1	0	0	0.04	0.02	0.07
N	H^N	0.99	0.03	0	0	0	0.07	0.04	0.11
		1.00	0.00	0	45	1	0.07	0.03	0.10
		1.00	0.01	0	46	90	0.05	0.03	0.07
		1.00	0.03	0	45	180	0.06	0.03	0.08
		1.00	0.01	0	45	270	0.06	0.04	0.07
		0.99	0.01	0	90	1	0.04	0.02	0.08
		1.01	0.01	0	90	45	0.04	0.02	0.06
		1.01	0.01	0	90	90	0.06	0.04	0.08
		0.99	0.01	0	90	135	0.05	0.03	0.08

[a] Pairs of nuclei for which dipolar couplings are computed. [b] Ratio of the best fitting and the predefined tensor size ($D_{zz} = 20$ Hz for $N-H^N$ couplings). [c] Rhombicities and [d,e,f] orientations of the predefined and back-calculated tensors. [g,h,i] Q_{all}, Q_{sec}, and Q_{loop} are the Q values (eq 1) for the whole protein, the secondary structural elements, and the loops, respectively.

5. Reconstructing Motional Distributions from Multiple Alignment Data

From the previous analysis, it becomes clear that static and motional contributions to a dipolar coupling measured for a single alignment cannot readily be separated. The questions are addressed here of how this task can be accomplished by combining dipolar couplings measured for different alignment tensors and what aspects of the motional distributions of the internuclear vectors can be reconstructed.

For this purpose, five $N-H^N$ pairs were selected in ubiquitin that show differential motional properties: Ala 28 (α helix) and Ile 44 (β sheet), which are part of regular secondary structures, and Lys 11, Ile 36, and Asp 52, which belong to the more mobile loop regions. The distinct motional behavior of these residues in the MD trajectory is reflected in their φ,ψ dihedral angle fluctuations. The right column in Figure 4 shows the φ,ψ distributions for the 500 MD snapshots: Ala 28 and Ile 44 show quite narrow φ,ψ distributions characteristic of α helix and β sheet structures, while Lys 11 and Ile 36 exhibit significantly wider distributions, in particular in their φ dihedral angle. Asp 52 exhibits a less regular behavior, indicative of a multimodal distribution. Dipolar couplings are sensitive to reorientations related to fluctuations of nearby dihedral angles as well as to longer range motions related to fluctuations of dihedral angles that are farther away.

In the left and middle panels of Figure 4, the orientations of the above-mentioned $N-H^N$ vectors are displayed for the 500 MD snapshots indicated as dots as a function of the polar angles (θ,φ). The orientational distributions of the 500 snapshots are in all cases elongated (approximately elliptical for Ala 28 and Ile 44); i.e., they do not exhibit axial symmetry. The large filled circle in the center of each panel represents the orientation of the $N-H^N$ vector in the average structure. The superimposed solid lines represent $N-H^N$ vector orientations that are consistent with the dipolar couplings averaged over the 500 snapshots for the nine different alignment tensors with $R = 0$ described in the previous section (see Tables 2 and 3). Thus, any static $N-H^N$ vector that points along a (θ,φ) direction belonging to a certain line could accurately reproduce the (scaled) dipolar coupling averaged over the trajectory for the alignment tensor associated with this line.

The panels in the left column correspond to scenario II, with the fitted alignment tensors given in the lower part of Table 2, while the panels in the middle column correspond to scenario III, where the couplings were divided by their individual S_{LS} order parameter. If all nine lines intersect at a single point, then a static $N-H^N$ vector pointing along the intersection can simultaneously reproduce all MD-averaged couplings for the nine alignments. For the regular secondary structural residues Ala 28 and Ile 44, this behavior is approximately found for scenario II (left column of Figure 4), while it is not fulfilled for the three other residues, Lys 11, Ile 36, and Asp 52. For the latter residues, MD-averaged dipolar couplings measured for multiple alignments cannot be quantitatively reproduced by a static structural model.

Individual S_{LS} scaling of dipolar couplings (scenario III, middle column of Figure 4) improves the situation, in particular for Ala 28 and Ile 44, which belong to regular secondary structures although the reorientational distributions of these vectors are not axially symmetric. For these vectors, the intersections coincide with the dipolar coupling predicted from the average structure (filled circle). Thus, the MD-averaged dipolar couplings obtained in multiple alignment media scaled by their respective S_{LS} values allow for these residues the reconstruction of highly accurate average orientations. For a set of dipolar coupling measurements performed for a sufficiently large number of different alignments (five or more), it is conceivable to use an effective dipolar scaling factor $\lambda_{rdc,eff}$ as a fitting parameter. Since $\lambda_{rdc,eff}$ covers besides the relaxation-

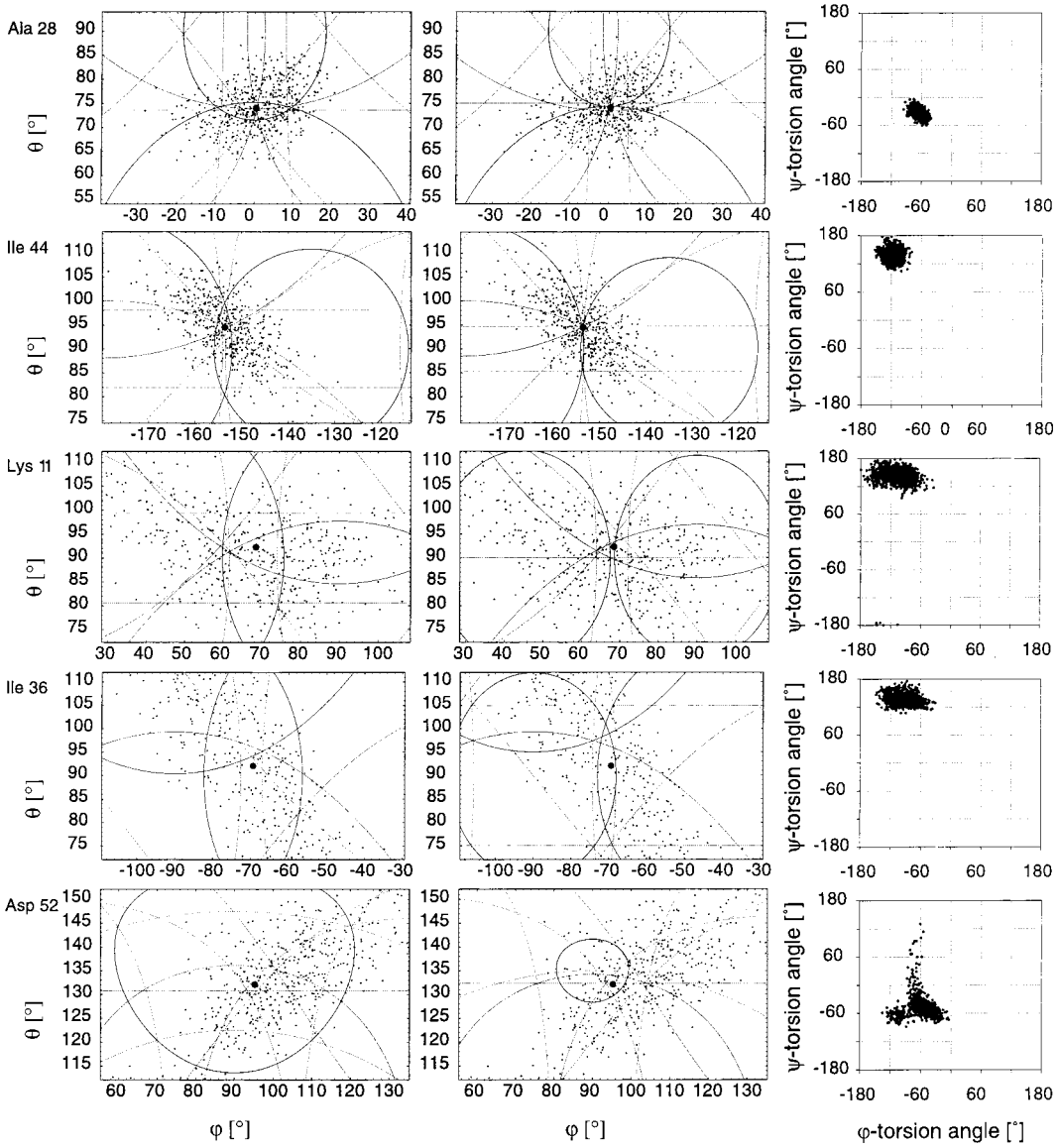

Figure 4. Determination of average $N-H^N$ directions from dipolar couplings measured for nine different alignment tensors exemplified for residues Ala 28, Ile 44, Lys 11, Ile 36, and Asp 52. The dots in the panels in the left and the middle columns correspond to the orientations of the $N-H^N$ vectors of 500 snapshots in the selected angular ranges. The full distributions are displayed on the spheres of Figure 1. The solid lines represent all static orientations that reproduce the MD-averaged couplings for the corresponding alignment tensors. The left panel corresponds to scenario II (no individual scaling of couplings), while the middle panel corresponds to scenario III (each coupling is scaled by its Lipari−Szabo order parameter S_{LS}). The panels in the right column show the φ,ψ dihedral angle distributions for these residues.

active motional time scales also slower time scales, comparison of $\lambda_{rdc,eff}$ with experimentally determined S_{LS} parameters should allow one to gain important insight into intramolecular motions occurring between nanosecond and millisecond time scales. It is expected that generally $\lambda_{rdc,eff} \leq S_{LS}$.

In contrast, for the mobile residues Lys 11, Ile 36, and Asp 52, none of the scenarios yields satisfactory results for the average orientations (left and middle columns of Figure 4). For scenario III (middle column), scaling by S_{LS} somewhat narrows down the range of possible average orientations, but obviously simple scaling remains insufficient for a quantitative determination of the average orientations because of the mathematical inequivalence of S_{LS} and λ_{rdc} for non-axially symmetric orientational distributions (cf. eqs 7, 9, and 12). Since according to eqs 7 and 9 λ_{rdc} directly depends on the average orientation of the dipolar vector, extraction of the average orientation and of the motional averaging effects becomes more complicated.

Model-Free Extraction of $\langle Y_{2M}\rangle$ and (θ_{eff},φ_{eff}) Quantities. The following two-step procedure is proposed using experimental dipolar couplings and S_{LS} order parameters:

1. Absolute alignment tensors **D** for multiple liquid-crystalline media are determined from experimental dipolar couplings using S_{LS} order parameters obtained from relaxation experiments for residues belonging to well-defined secondary structures.

2. The average orientation of a dipolar vector belonging to a more mobile region is extracted by fitting the averaged spherical harmonics $\langle Y_{2M}\rangle$, $M = -2, -1, 0, 1, 2$, to the dipolar couplings collected in all available alignment media using eq 9 with **D** of 1 and by determining the orientations (θ_{eff},φ_{eff}) by a least-squares fit according to eq 10.

The averaged spherical harmonics $\langle Y_{2M}\rangle$ quantities provide a "model-free" representation of motional effects on dipolar couplings in analogy to S^2_{LS} order parameters in spin relaxation studies.[21] In fact, the $\langle Y_{2M}\rangle$ quantities contain information about

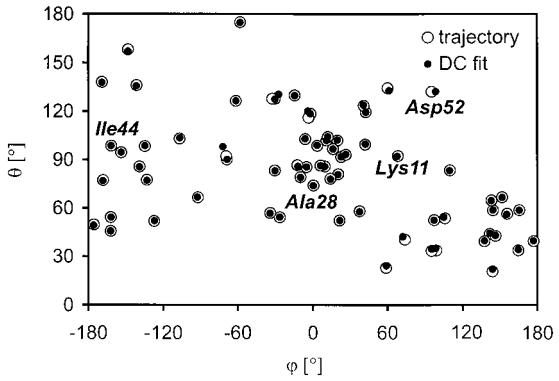

Figure 5. Comparison between average $N-H^N$ directions $(\theta_{av},\varphi_{av})$ determined from the MD trajectory and estimates $(\theta_{eff},\varphi_{eff})$ determined by solving the linear system of equations (eq 9) followed by the minimization of the sum of eq 10. The figure shows that the estimate is generally within 2° of the exact average.

motional asymmetry, which has become lost in S^2_{LS}. The above procedure was applied to the MD-averaged dipolar couplings, with results shown in Figures 5 and 6. Comparison between average $N-H^N$ directions $(\theta_{av},\varphi_{av})$ computed from the MD trajectory and estimates $(\theta_{eff},\varphi_{eff})$ determined by solving the overdetermined linear system of equations (eq 9), including the residual dipolar couplings determined for all nine alignment media, followed by the minimization of the sum of eq 10, yields differences that are less than 2° for residues in secondary structural elements (Figure 5). Although the deviation can be larger for loop regions (up to 5°), the $(\theta_{eff},\varphi_{eff})$ values provide, on average, a much better and more reliable estimate for $(\theta_{av},\varphi_{av})$ than the (θ,φ) values that are consistent with a single dipolar coupling value. From the extracted $\langle Y_{2M}\rangle$ quantities S^2_{rdc} values were determined according to eq 12. As expected, they turn out to be identical with the S^2_{LS} values determined directly from the trajectory.

Furthermore, asymmetry parameters η, which reflect the amount of asymmetry in reorientational motion (eq 11), were determined from the extracted $\langle Y_{2M}\rangle$ quantities, and they are shown in Figure 6 as a function of the amino acid number. The largest asymmetry is found in ubiquitin for residues in mobile loop regions with η values exceeding 10% (see Figure 6), while in secondary structural elements the asymmetry is typically well below 5%.

6. Conclusion

Intramolecular motions affect residual dipolar couplings in the form of a scaling by a factor λ_{rdc}, which generally also depends on the average orientation of the internuclear vector with respect to the alignment frame. Using a MD simulation as a reference, motional averaging effects of dipolar couplings have been described in detail, and a solution to the inverse problem has been presented that used theoretical dipolar couplings, assuming an optimal set of different alignment tensors. The proposed self-consistent analysis of dipolar couplings should allow the extraction of accurate structural information in terms of average orientations also when applied to experimental data.

Alignment tensors that are fitted to dipolar couplings tend to absorb a significant amount of intramolecular motional effects. If no information on S_{LS} order parameters is available, refinement of a static structural model should be "stopped" at Q values of about 0.05 for secondary structural parts and of about 0.1 for more mobile loop regions. If S_{LS} values are available, refinement to smaller Q values is conceivable, provided that no slower time scale motions are present.

Information on such slower time scale motions that are not reflected in spin relaxation data can be obtained from dipolar couplings measured in different liquid-crystalline media. The results presented here suggest that the combined use of dipolar coupling data sets measured in five or more different environments allows the accurate reconstruction of average positions and the retrieval of unique information on motional averaging of spherical harmonic functions of rank 2, $\langle Y_{2M}\rangle$, that is not readily accessible by S^2_{LS} order parameters obtained from spin relaxation measurements. Besides the longer time scales probed by dipolar couplings, also direct information about motional asymmetry of individual internuclear vectors, expressed by the parameter η, is available. For rapid axially symmetric reorientational motion of an internuclear vector, λ_{rdc} becomes equal to S_{rdc}. The $\langle Y_{2M}\rangle$ quantities have a "model-free" character similar to the model-free order parameters S^2_{LS} extracted from NMR spin relaxation experiments.[21] In analogy to the NMR relaxation field, interpretation of the $\langle Y_{2M}\rangle$ quantities in terms of concrete motional models, such as the 3D GAF model,[30] is possible as a subsequent step of data interpretation.

The basic assumption made here is that the liquid-crystalline environment does not affect biomolecular structure and dynamics. This assumption can be experimentally tested to some extent by verifying that chemical shifts, line widths, and homo- and heteronuclear relaxation parameters do not significantly change with the liquid-crystalline environment. In the case that the average protein structure varies for different alignment media, such variations would be reflected also in the $\langle Y_{2M}\rangle$ quantities.

At present, the requirement of five different liquid-crystalline environments may seem demanding. Moreover, the different alignment tensors should significantly differ with respect to each other in order to minimize the influence of experimental uncertainties in the residual dipolar couplings. Rapid progress in the development and understanding of aligning tools, however, makes it likely that soon a sufficient number of different alignment media will become available that lead to different alignment tensors.[4,5,34−52] Application of the presented protocol to experimental data is currently under way.

After submission of this work, a paper by Tolman et al.[53] appeared, in which the effects of protein motions on dipolar

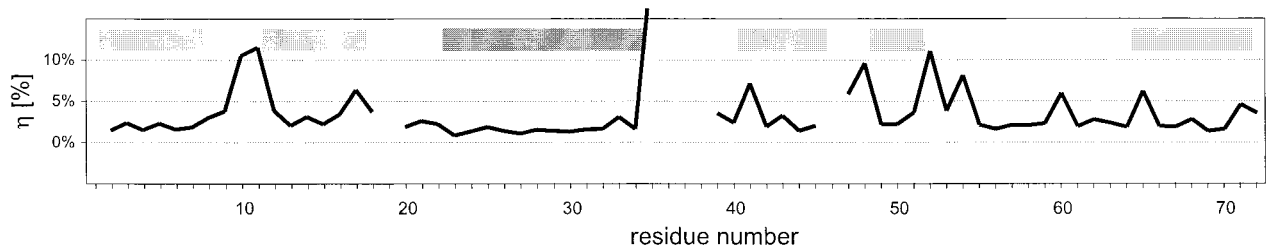

Figure 6. Motional asymmetry parameter η defined in eq 11 for $N-H^N$ vectors as a function of the residue number. In regular secondary structure, η varies between 1% and 6%, while in more mobile loop regions the asymmetry can exceed 10%.

couplings measured for a single alignment tensor in ubiquitin were discussed. It differs from the one presented here in the following way. In the paper by Tolman et al., experimental dipolar couplings of different vectors in the peptide plane measured for one alignment medium were interpreted using analytical motional models, whereas in the present work MD-generated dipolar couplings of a single vector measured in multiple alignments were interpreted in a "model-free" way.

Acknowledgment. The authors thank reviewers for useful comments. This work was initiated during J.M.'s stay at Clark University. J.M. and W.P. are recipients of a Kekulé doctoral fellowship of the Fonds der chemischen Industrie, and J.J.P. is a recipient of a Human Frontier Science Program postdoctoral fellowship. This work was supported by the DFG, MPG, the Fond der chemischen Industrie (to C.G.), and NSF Grant MCB-9904875 (to R.B.).

Supporting Information Available: Two tables with structural and dipolar coupling averaging information determined from the 10 ns trajectory of ubiquitin; figure exemplifying the effect of errors in the dipolar couplings on the extraction of motional and structural information (PDF). This material is available free of charge via the Internet at http://pubs.acs.org.

JA010002Z

(34) Prosser, S. R.; Losonczi, J. A.; Shiyanovskaya, I. V. *J. Am. Chem. Soc.* **1998**, *120*, 11010−11011.
(35) Barrientos, L. G.; Dolan, C.; Gronenborn, A. M. *J. Biomol. NMR* **2000**, *16*, 329−337.
(36) Clore, G. M.; Starich, M. R.; Gronenborn, A. M. *J. Am. Chem. Soc.* **1998**, *120*, 10571−10572.
(37) Hansen, M. R.; Mueller, L.; Pardi, A. *Nat. Struct. Biol.* **1998**, *5*, 1065−1074.
(38) Hansen, M. R.; Rance, M.; Pardi, A. *J. Am. Chem. Soc.* **1998**, *120*, 11210−11211.
(39) Ojennus, D. D.; Mitton-Fry, R. M.; Wuttke, D. S. *J. Biomol. NMR* **1999**, *14*, 175−179.
(40) Ottiger, M.; Bax, A. *J. Biomol. NMR* **1998**, *12*, 361−372.
(41) Ottiger, M.; Bax, A. *J. Biomol. NMR* **1999**, *13*, 187−191.
(42) Sanders, C. R.; Schwonek, J. P. *Biochemistry* **1992**, *31*, 8898−8905.
(43) Sanders, C. R.; Hare, B. J.; Howard, K. P.; Prestegard, J. H. *Prog. NMR Spectrosc.* **1994**, *26*, 421−444.
(44) Wang, H.; Eberstadt, M.; Olejniczak, T.; Meadows, R. P.; Fesik, S. W. *J. Biomol. NMR* **1998**, *12*, 443−446.
(45) Cavagnero, S.; Dyson, J. H.; Wright, P. E. *J. Biomol. NMR* **1999**, *13*, 387−391.
(46) Losonczi, J. A.; Prestegard, J. H. *J. Biomol. NMR* **1998**, *12*, 447−451.
(47) Ruckert, M.; Otting, G. *J. Am. Chem. Soc.* **2000**, *122*, 7793−7797.
(48) Flemming, K.; Gray, D.; Prasannan, S.; Matthews, S. *J. Am. Chem. Soc.* **2000**, *122*, 5224−5225.
(49) Tycko, R.; Blanco, F. J.; Ishii, Y. *J. Am. Chem. Soc.* **2000**, *122*, 9340−9341.
(50) Sass, J.; Musco, G.; Stahl, S. J.; Wingfield, P. T.; Grzesiek, S. *J. Biomol. NMR* **2000**, *18*, 303−309.
(51) Koenig, B. W.; Hu, J.-S.; Ottiger, M.; Bose, S.; Hendler, R. W.; Bax, A. *J. Am. Chem. Soc.* **1999**, *121*, 1385−1386.
(52) Sass, J.; Cordier, F.; Hoffmann, A.; Rogowski, M.; Cousin, A.; Omichinski, J. G.; Lowen, H.; Grzesiek, S. *J. Am. Chem. Soc.* **1999**, *121*, 2047−2055.
(53) Tolman, J. R.; Al-Hashimi, H. M.; Kay, L. E.; Prestegard, J. H. *J. Am. Chem. Soc.* **2001**, *123*, 1416−1424.